

5-2001

Optical properties of $\text{RNi}_2\text{B}_2\text{C}$ (R=Y,Tb,Er,Dy)

S. J. Lee

Iowa State University

B. K. Cho

K-JIST

Paul C. Canfield

Iowa State University, canfield@ameslab.gov

David W. Lynch

Iowa State University, dlynch@iastate.edu

Follow this and additional works at: http://lib.dr.iastate.edu/physastro_pubs

 Part of the [Atomic, Molecular and Optical Physics Commons](#), and the [Condensed Matter Physics Commons](#)

The complete bibliographic information for this item can be found at http://lib.dr.iastate.edu/physastro_pubs/113. For information on how to cite this item, please visit <http://lib.dr.iastate.edu/howtocite.html>.

This Article is brought to you for free and open access by the Physics and Astronomy at Iowa State University Digital Repository. It has been accepted for inclusion in Physics and Astronomy Publications by an authorized administrator of Iowa State University Digital Repository. For more information, please contact digirep@iastate.edu.

Optical properties of RNi₂B₂C (R=Y,Tb,Er,Dy)

Abstract

The optical properties of single crystals of RNi₂B₂C (R=Y,Tb,Er, and Dy) were measured between 1.7 and 5.2 eV at room temperature using a spectroscopic ellipsometer. The spectra for all compounds are similar and the peak positions appear in a similar energy region. The similarity of the spectra of RNi₂B₂C (R=Tb,Er,Dy) to that of YNi₂B₂C indicates that the rare-earth 4f states are not actively involved in the optical transitions.

Keywords

Ames Laboratory, YNi₂B₂C, spectroscopic ellipsometer

Disciplines

Atomic, Molecular and Optical Physics | Condensed Matter Physics | Physics

Comments

This article is from *Physical Review B* 63 (2001): 233103, doi:[10.1103/PhysRevB.63.233103](https://doi.org/10.1103/PhysRevB.63.233103). Posted with permission.

Optical properties of $R\text{Ni}_2\text{B}_2\text{C}$ ($R = \text{Y, Tb, Er, Dy}$)

S. J. Lee

Ames Laboratory, Iowa State University, Ames, Iowa 50011

B. K. Cho

Department of Materials Science and Technology, K-JIST, Kwang-Joo, 500-712, Korea

P. C. Canfield and D. W. Lynch

Ames Laboratory and Department of Physics and Astronomy, Iowa State University, Ames, Iowa 50011

(Received 2 October 2000; revised manuscript received 9 March 2001; published 18 May 2001)

The optical properties of single crystals of $R\text{Ni}_2\text{B}_2\text{C}$ ($R = \text{Y, Tb, Er, and Dy}$) were measured between 1.7 and 5.2 eV at room temperature using a spectroscopic ellipsometer. The spectra for all compounds are similar and the peak positions appear in a similar energy region. The similarity of the spectra of $R\text{Ni}_2\text{B}_2\text{C}$ ($R = \text{Tb, Er, Dy}$) to that of $\text{YNi}_2\text{B}_2\text{C}$ indicates that the rare-earth $4f$ states are not actively involved in the optical transitions.

DOI: 10.1103/PhysRevB.63.233103

PACS number(s): 68.35.Ja, 71.20.-b, 71.20.Eh, 74.25.Gz

The magnetic, transport, and electrical properties of the magnetic superconductors $R\text{Ni}_2\text{B}_2\text{C}$ ($R = \text{rare earth, Y}$) have been investigated widely because they offer a system for studying the interaction of superconductivity with magnetism.¹⁻⁷ The crystal structure of $R\text{Ni}_2\text{B}_2\text{C}$ is the ThCr_2Si_2 type with additional carbon atoms in each R layer. Adding C atoms between boron-boron bonds results in the expansion of the lattice along the c axis and contraction along the a and b axes. As a result, the structure can be viewed as a layered system in geometrical structure, reminiscent of the high- T_c oxide superconductors. A series of papers on band structure calculations on $\text{LuNi}_2\text{B}_2\text{C}$ and $\text{YNi}_2\text{B}_2\text{C}$ have been published, concluding that the electronic properties are three dimensional rather than two dimensional.⁸⁻¹² However, there have been no band structure calculations reported on samples with R other than Y and Lu, in which the $4f$ shell is not completely closed, because the local density approximation (LDA) does not treat well the strong correlations of the localized $4f$ electrons in the unfilled $4f$ shell. Therefore, the optical experimental data presented in this paper provide useful information on the electronic structure for compounds with an unfilled $4f$ shell.

The optical conductivity and dielectric function for $\text{LuNi}_2\text{B}_2\text{C}$ and $\text{YNi}_2\text{B}_2\text{C}$ have been studied to understand the mechanism of superconductivity in these materials. Bommeli *et al.*¹³⁻¹⁵ identified a superconducting gap of 5.6 and 6.9 meV for $\text{LuNi}_2\text{B}_2\text{C}$ and $\text{YNi}_2\text{B}_2\text{C}$, respectively, by measuring the far-infrared optical reflectivity at 6 K. They concluded that the superconducting mechanism for Lu and Y compounds can be understood within the framework of conventional BCS theory.

From the density of states at the Fermi energy, the experimental value of the electronic heat coefficient (γ) and coupling constant (λ) can be obtained. These can be used for studying the mechanism of superconductivity in the compound. The large value of the mass enhancement factor for $\text{LuNi}_2\text{B}_2\text{C}$ and $\text{YNi}_2\text{B}_2\text{C}$ indicates a conventional BCS mechanism for the superconductivity. The mass enhancement factor arises due to the electron-electron and electron-

phonon interactions. The electron-phonon interaction increases the transition temperature while the electron-electron interaction reduces the transition temperature, that is, the electron-electron interaction acts against superconductivity. The electron-electron interaction can be obtained from experimental data on the isotope shift coefficient of a superconductor and is usually taken to be between 0.1 and 0.15.^{10,12,16,17} Using these values and the renormalized Bardeen-Cooper-Schrieffer formula or McMillan's formula,¹⁶ the estimated electron-phonon coupling constants for $\text{LuNi}_2\text{B}_2\text{C}$ and $\text{YNi}_2\text{B}_2\text{C}$ are between 0.8 and 1.1,^{12,17} which indicates that the superconductivity in $\text{LuNi}_2\text{B}_2\text{C}$ and $\text{YNi}_2\text{B}_2\text{C}$ can be described by the conventional phonon mechanism.

Bommeli *et al.* also found that the structural anisotropy does not affect the optical data because polycrystalline and single crystalline samples produced equivalent experimental results. This is consistent with the band structure calculation, suggesting that these are electronically three-dimensional even though they have layered crystal structures.¹⁸ Widder *et al.*^{19,20} obtained the dielectric function of $\text{YNi}_2\text{B}_2\text{C}$ by linking optical reflectance and electron energy loss measurements. They applied a sum rule to the free-carrier contribution to the optical conductivity and obtained an unscreened plasmon energy of $\hbar\omega = 4.25$ eV.

$\text{YNi}_2\text{B}_2\text{C}$ is a good reference system for studying the physical properties of the $R\text{Ni}_2\text{B}_2\text{C}$ series because Y $4f$ states are empty and located far above the Fermi level E_F and do not affect the physical properties of $\text{YNi}_2\text{B}_2\text{C}$. We measured optical data on a single crystal of $\text{YNi}_2\text{B}_2\text{C}$ and analyzed the optical response in the visible and UV region using the electronic structure of $\text{YNi}_2\text{B}_2\text{C}$. The optical spectra of $R\text{Ni}_2\text{B}_2\text{C}$ ($R = \text{Tb, Er, Dy}$) were also measured and compared to those of $\text{YNi}_2\text{B}_2\text{C}$.

Polycrystalline stoichiometric $R\text{Ni}_2\text{B}_2\text{C}$ ($R = \text{Y, Tb, Er, Dy}$) compounds were synthesized by arc-melting together high-purity Y, Tb, Er, Dy (Ames Laboratory, 99.99%), Ni (99.95%), B (99.5%), and C (99.99%) under argon gas on a water-cooled copper hearth. An excess of

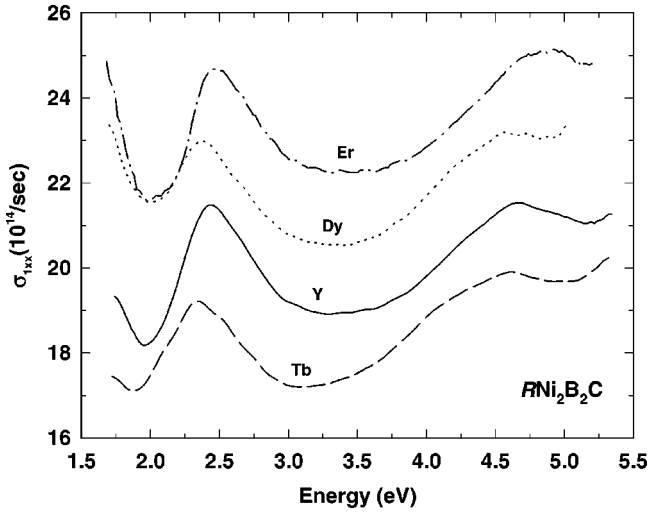


FIG. 1. The real part of the complex optical conductivity of $R\text{Ni}_2\text{B}_2\text{C}$ ($R = \text{Y, Tb, Dy, Er}$) measured at room temperature with no applied magnetic field.

5 wt % of B over that required for stoichiometry was added to the stoichiometric mixture to compensate the loss of mass during arc melting. Single crystals were then grown from the polycrystalline bulk sample by a high-temperature flux method using Ni_2B as a solvent.^{21,22} Powder x-ray diffraction patterns of pulverized single crystals could be indexed well with the known structure type, indicating a single phase. The most intense (211) line of Ni_2B was seen and is due to small amounts of flux remaining on the surface of the grown crystals. The crystals separated from the flux are platelike with the crystallographic c axis perpendicular to the plate surface. The crystal surface was polished to remove the remaining flux and to make the surface mirrorlike for optical measurements.

Ellipsometry is widely used to characterize surfaces, interfaces, and thin films. The principle of ellipsometry is that the state of polarization of light is changed on reflection. This change is directly related to the dielectric function of the reflecting material. With rotating analyzer ellipsometry²³ one measures the complex reflectivity ratio

$$\rho = \frac{r_p}{r_s} = \left| \frac{r_p}{r_s} \right| e^{i\Delta} = \tan \Psi e^{i\Delta}, \quad (1)$$

where r_p and r_s are the complex amplitude reflection coefficients for p and s polarized light, and Ψ and Δ express the change in amplitude and phase between p and s components of the polarized light reflected from a surface. Ψ and Δ are quantities directly measurable by ellipsometry. The complex dielectric function $\tilde{\epsilon}$ is related to the complex reflectivity ratio $\tilde{\rho}$ by

$$\tilde{\epsilon} = \sin^2 \phi_0 + \sin^2 \phi_0 \tan^2 \phi_0 \left[\frac{1 - \tilde{\rho}}{1 + \tilde{\rho}} \right]^2, \quad (2)$$

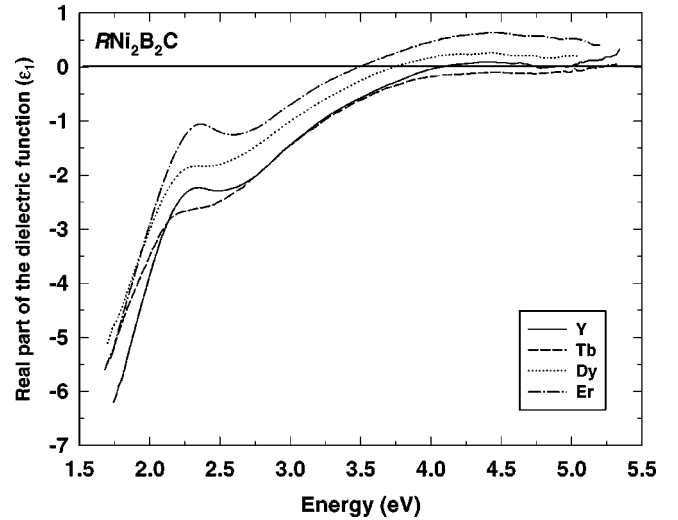


FIG. 2. The real part of the complex dielectric function of $R\text{Ni}_2\text{B}_2\text{C}$ ($R = \text{Y, Tb, Dy, Er}$).

where ϕ_0 is the angle of incidence, which is 68° in this experiment. From the complex dielectric function $\tilde{\epsilon}$, the complex optical conductivity $\tilde{\sigma}$ can be obtained from

$$\tilde{\epsilon} = 1 - \frac{4\pi\tilde{\sigma}i}{\omega}. \quad (3)$$

The absorptive part of the optical conductivity σ_1 is related to the imaginary part of the dielectric function ϵ_2 by

$$\sigma_1 = \frac{\omega\epsilon_2}{4\pi}. \quad (4)$$

The spectrum of the optical conductivity for $\text{YNi}_2\text{B}_2\text{C}$ is plotted as a solid line together with those for $R\text{Ni}_2\text{B}_2\text{C}$ ($R = \text{Tb, Dy, Er}$) in Fig. 1. There are two peaks in the optical spectra for all compounds. The first peak is between 2.3 and 2.5 eV and the second, which is weaker and broader than the

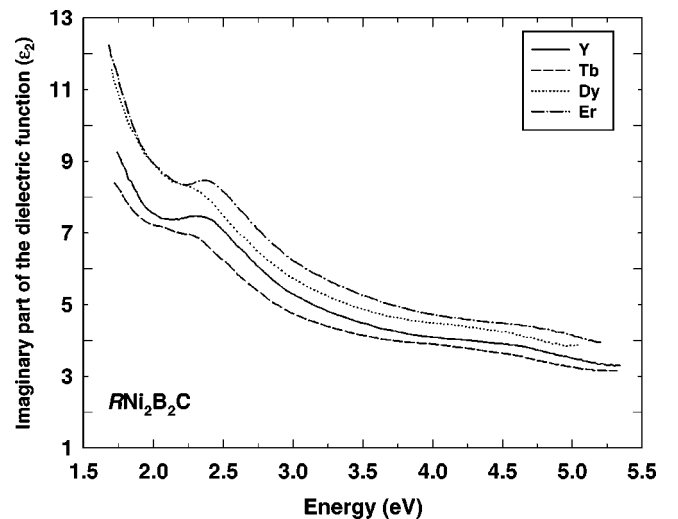


FIG. 3. The imaginary part of the complex dielectric function of $R\text{Ni}_2\text{B}_2\text{C}$ ($R = \text{Y, Tb, Dy, Er}$).

first peak, appears between 4.5 and 5.0 eV. For the first peak of $\text{YNi}_2\text{B}_2\text{C}$ at 2.4 eV, the occupied Ni 3*d* states and the unoccupied Ni 4*p* states are expected to be involved in the transitions from analysis of the band structure calculation.^{10,11} The second peak at 4.6 eV may involve contributions from the occupied Y 5*p* states to the empty Y 4*d* states located broadly between 4 and 6 eV. The second peak in $\text{YNi}_2\text{B}_2\text{C}$ was not clearly observed in the measurement of Bommeli *et al.*^{13–15} and of Widder *et al.*^{19,20} who used a Kramers-Kronig transformation of the reflectivity to obtain the optical conductivity. The first peak was observed in the measurement of Widder *et al.*^{19,20} and weakly observed by Bommeli *et al.*^{13–15}

The origin of the first peak for $R\text{Ni}_2\text{B}_2\text{C}$ ($R = \text{Tb, Dy, Er}$) is expected to be similar to that of $\text{YNi}_2\text{B}_2\text{C}$ because the peak positions and shapes are similar. The second peak for Tb, Dy, and Er compounds is mainly caused by the contribution of the *R* 5*d* states of the compounds. The real part of the complex dielectric function is shown in Fig. 2. The large negative curve in the figure is due to the large free-electron gas contribution to ϵ_1 . The first peak in the ϵ_1 spectra is due to interband transitions. The zero crossing of ϵ_1 for

$\text{YNi}_2\text{B}_2\text{C}$ occurs at 4.0 eV. This is lower than the unscreened plasma energy obtained by Widder *et al.*¹⁹ by 0.25 eV, because it is shifted by the interband contribution. The imaginary part of the dielectric function, which can be derived from the real part of the optical conductivity by using Eq. (4), is shown in Fig. 3. Interband contributions to the dielectric function appear between 2.3 and 2.5 eV and weak peaks appear between 4.5 and 5.0 eV.

In summary, we have measured the optical conductivity spectra of $R\text{Ni}_2\text{B}_2\text{C}$ ($R = \text{Y, Tb, Er, Dy}$) at room temperature using spectroscopic ellipsometry. The spectra for all compounds are similar and the peak positions appear in a similar energy region. The similarity of the spectra of $R\text{Ni}_2\text{B}_2\text{C}$ ($R = \text{Tb, Er, Dy}$) to that of $\text{YNi}_2\text{B}_2\text{C}$ indicates that the rare-earth 4*f* states are not actively involved in the optical transitions in the measured photon energy range.

Ames Laboratory is operated for the U.S. Department of Energy by Iowa State University under Contract No. W-7405-Eng-82. This work was supported by the Director of Energy Research, Office of Basic Energy Science. The work at K-JIST was supported by the Brain Korea 21 project.

-
- ¹R.J. Cava, H. Takagi, B. Batlogg, H.W. Zandbergen, J.J. Krajewski, W.F. Peck, Jr., R.B. van Dover, R.J. Felder, T. Siegrist, K. Mizuhashi, J.O. Lee, H. Eisaki, S.A. Carter, and S. Uchida, *Nature (London)* **367**, 146 (1994).
- ²R.J. Cava, H. Takagi, H.W. Zandbergen, J.J. Krajewski, W.F. Peck, Jr., T. Siegrist, B. Batlogg, R.B. van Dover, R.J. Felder, K. Mizuhashi, J.O. Lee, H. Eisaki, and S. Uchida, *Nature (London)* **367**, 252 (1994).
- ³M.O. Mun, S.I. Lee, and W. C. Lee, *Phys. Rev. B* **56**, 14 668 (1995).
- ⁴I.R. Fisher, J.R. Cooper, and P.C. Canfield, *Phys. Rev. B* **56**, 10 920 (1997).
- ⁵T. Terashima, C. Haworth, H. Takeya, S. Uji, H. Aoki, and K. Kadowaki, *Phys. Rev. B* **56**, 5120 (1997).
- ⁶M. Bullock, J. Zarestky, C. Stassis, A. Goldman, P. Canfield, Z. Honda, G. Shirane, and S. M. Shapiro, *Phys. Rev. B* **57**, 7916 (1998).
- ⁷V.N. Narozhnyl, J. Feudenberger, V.N. Kochetkov, K.A. Nenkov, G. Fuchs, A. Handstein, and K.-H. Müller, *Phys. Rev. B* **59**, 14 762 (1999).
- ⁸W.E. Pickett and D.J. Singh, *Phys. Rev. Lett.* **72**, 3702 (1994).
- ⁹L.F. Mattheiss, *Phys. Rev. B* **49**, 13 279 (1994).
- ¹⁰J.I. Lee, T.S. Zhao, I.G. Kim, B.I. Min, and S.J. Youn, *Phys. Rev. B* **50**, 4030 (1994).
- ¹¹J.K. Burdett and S. Sevov, *Inorg. Chem.* **33**, 3857 (1994).
- ¹²H. Kim, C.D. Hwang, and J. Ihm, *Phys. Rev. B* **52**, 4592 (1995).
- ¹³F. Bommeli, L. Degiorgi, P. Wachter, B.K. Cho, P.C. Canfield, R. Chau, and M.B. Maple, *Phys. Rev. Lett.* **78**, 547 (1997).
- ¹⁴F. Bommeli, L. Degiorgi, P. Wachter, B.K. Cho, P.C. Canfield, R. Chau, and M.B. Maple, *Physica C* **282-287**, 1475 (1997).
- ¹⁵F. Bommeli, L. Degiorgi, P. Wachter, B.K. Cho, P.C. Canfield, R. Chau, and M.B. Maple, *Physica B* **230-232**, 879 (1997).
- ¹⁶W.L. McMillan, *Phys. Rev.* **167**, 331 (1968).
- ¹⁷K.D.D. Rathnayaka, A.K. Bhatnagar, A. Parasiris, and D.G. Naugle, *Phys. Rev. B* **55**, 8506 (1997).
- ¹⁸D.M. Poirier, C.G. Olson, D.W. Lynch, M. Schmidt, B.K. Cho, and P.C. Canfield, *J. Phys. Chem. Solids* **56**, 1881 (1995).
- ¹⁹K. Widdler, D. Berner, A. Zibold, H.P. Geserich, M. Knupfer, M. Kielwein, M. Buchgeister, and J. Fink, *Europhys. Lett.* **30**, 55 (1995).
- ²⁰K. Widder, M. Kielwein, M. Knupfer, J. Fink, D. Berner, H.P. Geserich, and K. Winzer, *J. Low Temp. Phys.* **105**, 1659 (1996).
- ²¹P.C. Canfield, P.L. Gammel, and D.J. Bishop, *Phys. Today* **51** (10), 40 (1998).
- ²²B.K. Cho, P.C. Canfield, L.L. Miller, W.P. Beyermann, and A. Yatskar, *Phys. Rev. B* **52**, 3684 (1995).
- ²³D.E. Aspnes and A.A. Studna, *Appl. Opt.* **14**, 220 (1975).